Int. J. Electrochem. Sci., 11 **(2016)** 7163 – 7172, doi: 10.20964/2016.08.66

International Journal of
ELECTROCHEMICAL
SCIENCE
www.electrochemsci.org

Microstructural Change and Corrosion Behavior During Rolling of Zr-based Bulk Metallic Glass

W. Zhou[*], *J.X. Hou, M.Q. Sheng*[*]

Shagang School of Iron and Steel, Soochow University, Suzhou 215021, China
[*]E-mail: wzhou@suda.edu.cn (W. Zhou), shengminqi@suda.edu.cn (M.Q. Sheng)

Received: 15 April 2016 / *Accepted:* 16 June 2016 / *Published:* 7 July 2016

Microstructural change and corrosion behavior of $Zr_{62}Cu_{12.5}Ni_{10}Al_{7.5}Ag_8$ bulk metallic glass (BMG) subjected to rolling at room temperature were studied. It is found that no phase transformation occurs, even when the BMG is rolled up to 95% reduction in thickness, except for the formation of narrow shear bands. Rolling-induced free volume in the BMG increases with the degree of deformation, which causes the decrease of corrosion potential and the increase of corrosion current density during the polarization of deformed BMG. It is proposed that the shear bands acting as preferential sites for pitting initiation, in which free volume is mainly stored, accounts for the reduction of corrosion resistance of BMG. However, the corrosion resistance in the rolled specimen can be improved by relaxation annealing associated with the annihilation of free volume.

Keywords: Zr-based bulk metallic glass; rolling deformation; free volume; corrosion resistance

1. INTRODUCTION

Bulk metallic glasses (BMGs) with long-range atomic disorder possess exotic properties such as high strength and hardness, excellent magnetic properties and corrosion resistance [1-6]. Nevertheless, they are metastable in thermodynamics. Under the heat treatment or mechanical deformation, microstructure change in the BMGs may take place due to the enhancement of atomic diffusion, leading to the absence of all the characteristic properties [7]. Therefore, it is important to examine the structural stability against plastic deformation for their safe applications. In this regard, a series of deformation-induced microstructure changes such as phase separation or crystallization and its effects on mechanical properties have been reported in some BMG systems [8-11]. But very little attention has been paid to the effect of deformation-induced microstructure change on the corrosion behavior of the BMG. Considering that their applications as engineering materials require long-term

environmental stability, it is worthwhile to scrutinize the corrosion resistance of deformed BMGs. In this work, a series of rolling deformation experiments were carried out on novel $Zr_{62}Cu_{12.5}Ni_{10}Al_{7.5}Ag_8$ BMG with excellent plasticity, and the changes in microstructure and corrosion behavior with deformation degree were systematically studied, which is important for both fundamental research and technological application of BMGs.

2. EXPERIMENT

Master alloy ingots with nominal composition of $Zr_{62}Cu_{12.5}Ni_{10}Al_{7.5}Ag_8$ were prepared by arc melting a mixture of pure Zr(99.9%), Al(99.99%), Ni(99.99%), Cu(99.99%), and Ag(99.99%) in a purified argon atmosphere. After six times remelting, the BMGs were producd by suction-casting for 60 mm long rectangular plates with a thickness of 1 mm and width of 10 mm. The plates were then cut into strips with 3 mm in width for rolling. Strain is denoted by thickness reduction $\varepsilon = (h_0\text{-}h)/h_0$, where h_0 and h represented the specimen thickness before and after rolling, respectively. The strain rate was carefully controlled to be about 1×10^{-1} s^{-1}.

Thermo ARL X-ray diffractometer (XRD) with monochromatic Cu Kα radiation and JEOL JEM-2100F high-resolution transmission electron microscopy (HRTEM) were conducted to investigate the microstructures of the specimens. Thermal analyses were carried out on Perkin-Elmer Pyris Diamond differential scanning calorimeter (DSC) under a flow of high purity argon. Corrosion behaviors of the as-cast plates and the as-rolled specimens were evaluated by electrochemical polarization measurement, which were conducted in a three-electrode cell, consisting of a test specimen, a platinum counter electrode and a standard saturated calomel reference electrode (SCE). Before polarization scan, the specimen was immersed in the electrolytes of 3.5% NaCl solutions for 20 min until the open circuit potential became steady. The electrochemical polarization measurement was examined at a potential sweep rate of 2 mV/s. At least four electrochemical measurements were conducted for an alloy to obtain reliable results. Surface of the corroded specimens after electrochemical polarization measurement were carefully examined using scanning electron microscope (SEM).

3. RESULTS AND DISCUSSION

Rolling at the strain rate of 1×10^{-1} s^{-1}, the $Zr_{62}Cu_{12.5}Ni_{10}Al_{7.5}Ag_8$ BMG exhibits excellent ductility and can be rolled to different thickness reductions (ε), respectively. The highest ε achieved in our experiments is 95%, up to which no fracture occurs. Fig. 1 shows the XRD patterns of the as-cast and as-rolled specimens. All of them consist of two broad diffraction peaks without any detectable crystalline peak within the sensitivity of XRD.

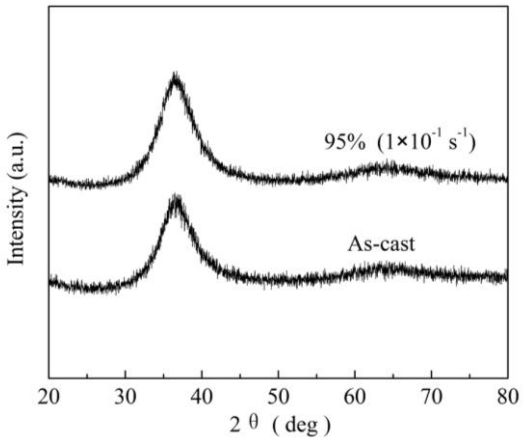

Figure 1. XRD patterns of the as-cast specimen and the specimen with 95% thickness reduction.

Fig. 2 displays the DSC traces of the as-cast and as-rolled specimens heating at 20 K/min. The as-cast specimen exhibits an endothermic event, which is characteristic of glass transition temperature T_g=648 K, followed by three exothermic reactions corresponding to the crystallization process with the first, second and third crystallization peak temperature (T_{p1}=745 K, T_{p2}=763 K and T_{p3}=783 K). The first exothermic reaction corresponds to formation of an icosahedral phase (I-phase) in the glass matrix, while the second and third one reflects the crystallization of the residual amorphous phase and the transformation of I-phase into the Zr_2Cu and Zr_2Ni intermetallic compounds [12], respectively. After rolling at 1×10^{-1} s^{-1}, as compared with the as-cast specimen, the peak temperatures and the corresponding enthalpies of the as-rolled specimens keep unchanged regardless of thickness reduction, indicating that no phase transformation takes place during the rolling deformation of BMG.

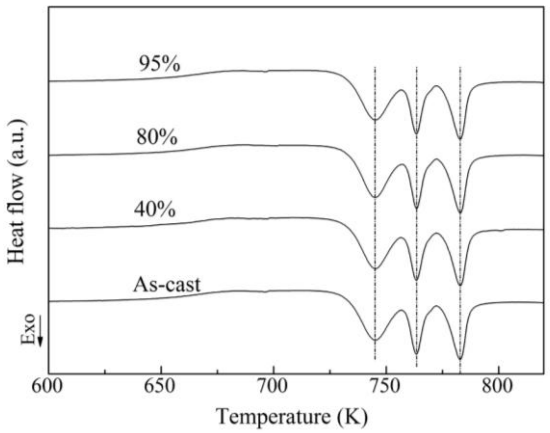

Figure 2. DSC curves of the specimens with different thickness reductions ε heating at 20 K/min.

HRTEM was carried out to carefully examine the microstructure of the as-cast and as-rolled specimens. As displayed in Figs. 3a and 3b, a homogeneous contrast in the bright-field image and a

diffraction halo in the selected area electron diffraction (SAED) pattern were found in the as-cast specimen, indicating the glassy nature of the alloy. Figs. 3c and 3d show the bright-field TEM image of specimen with ε=95% rolled at 1×10^{-1} s^{-1}. Compared with the undeformed specimen, no obvious contrast was observed except for a brighter shear band with about 5-10 nm in width. And no lattice fringes were observed inside or around the shear band, but the atomic configuration in the shear band becomes more disordered as compared with the undeformed matrix. The corresponding SAED pattern consists of a diffraction halo. These results further confirm the as-rolled specimens retain the amorphous structure, and neither phase separation nor nanocrystallization occurs during the rolling deformation.

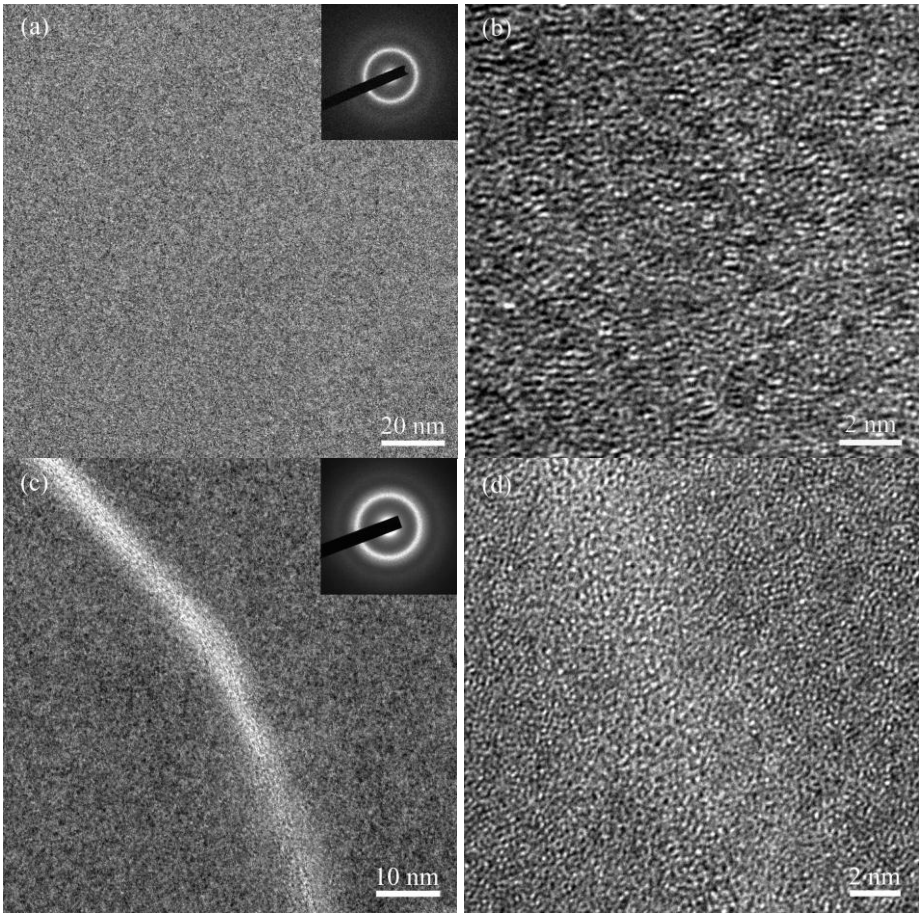

Figure 3. TEM bright-field images and the corresponding SAED patterns of the as-cast specimen (a) and the specimen with ε=95% rolled at 1×10^{-1} s^{-1} (c). (b, d) are the HRTEM images of (a) and (c), respectively.

The stable microstructure against deformation might be ascribed to the structural nature of metallic glasses. Dissimilar to crystals, metallic glasses do not possess long-range order while retain short or medium range order. The short or medium range order is however different from that of liquids. The microstructure of $Zr_{62}Cu_{12.5}Ni_{10}Al_{7.5}Ag_8$ BMG is heterogeneous, consisting of hard regions (IMRO) with less free volume and soft regions with more free volume [12]. The atoms in the

hard regions are closely packed with strong bonds, leading to high strength. While the weakly bonded soft regions with large free volume are characterized by low strength and are readily for the initiation of shear bands or plastic flow upon mechanical deformation. As has been argued, mechanical deformation tends to enhance the atomic mobility, which may consequently promote the change in microstructure. During the rolling of $Zr_{62}Cu_{12.5}Ni_{10}Al_{7.5}Ag_8$ BMG, however, the energy imposed by the rolling at 1×10^{-1} s^{-1} is not high enough to initiate the breaking and reforming of the strong bonds in the hard region. As a result, no amorphous-to-crystal phase transformation occurs, except for leading to some localized narrow shear bands in the soft regions.

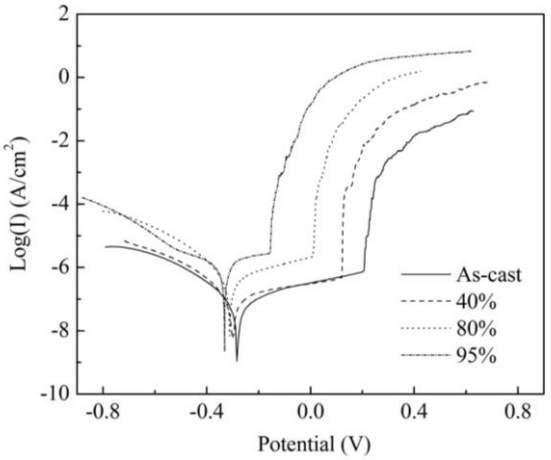

Figure 4. Polarization curves of the specimens with different ε at the strain rate of 1×10^{-1} s^{-1} in 3.5wt% NaCl solution open to air at room temperature.

Table 1. The corrosion potential E_{corr}, pitting potential E_{pit}, passive region E_{pit}-E_{corr}, and corrosion current density I_{corr} derived from the polarization curves for the $Zr_{62}Cu_{12.5}Ni_{10}Al_{7.5}Ag_8$ alloys.

Alloys	E_{corr} (mV)	E_{pit} (mV)	E_{pit}-E_{corr} (mV)	I_{corr} (A·cm^{-2})
As-cast	-284 ± 3	208 ± 2	492 ± 2	$(7.5 \pm 0.6) \times 10^{-8}$
40%	-301 ± 2	121 ± 2	422 ± 2	$(1.4 \pm 0.3) \times 10^{-7}$
80%	-312 ± 2	11 ± 1	323 ± 2	$(5.5 \pm 0.4) \times 10^{-7}$
95%	-332 ± 2	-156 ± 2	176 ± 2	$(1.3 \pm 0.3) \times 10^{-6}$
95%-annealed	-307 ± 2	86 ± 1	393 ± 2	$(2.2 \pm 0.3) \times 10^{-7}$

The polarization curves of the as-cast and as-rolled specimens in 3.5wt% NaCl solution open to air at room temperature are displayed in Fig. 4, and the derived corrosion parameters are presented in Table 1. It can be seen that the as-cast specimen spontaneously passivated with low current density (I_{corr}) of about 7.5×10^{-8} A·cm^{-2} prior to pitting corrosion (E_{pit}) at -208 mV. However, the polarization curves of the specimen subjected to rolling shifts to lower potential position, resulting in that the corrosion potential E_{corr} and E_{pit} become negative-shifting. Specifically, as ε increases from 0 to 95% during the rolling of BMG at the strain rate of 1×10^{-1} s^{-1}, the E_{corr} gradually decreases from -284 to -332 mV, and E_{pit} significantly decreases from -208 to -156 mV, making passive region E_{pit}-E_{corr}

decrease from 492 to 176 mV. Meanwhile, the I_{corr} tremendously decreases from 7.5×10^{-8} to 1.3×10^{-6} A·cm^{-2}. Generally, the higher E_{corr} and the lower I_{corr} reflect a better corrosion resistance. Therefore, it can be concluded that rolling deformation significantly reduces the corrosion resistance of BMG.

To further understand the influence of rolling deformation on the corrosion behavior of BMG, SEM was employed to investigate the morphologies. Fig. 5 displays the SEM images of the as-cast and as-rolled specimens anodically polarized to the potential at which pitting corrosion just took place. As is seen, the surface of the as-cast specimen appeared to be slightly corroded. Pitting corrosion occurred in some regions, where some corrosion products were formed. When the specimen rolled up to ε=60% at the strain rate of 1×10^{-1} s^{-1}, the pits produced are much larger in size than those in as-cast specimen. The preferential pitting initiation at shear bands can be obviously observed in the cross section of the specimen. The corrosion products were almost formed in the shear bands. However, a large number of pits, peel-like region and corrosion products can be observed for the specimens with ε=95%. These morphologies illustrate that rolling deformation deteriorates the corrosion resistance of the BMG, and pit corrosion preferentially initiates in the shear bands.

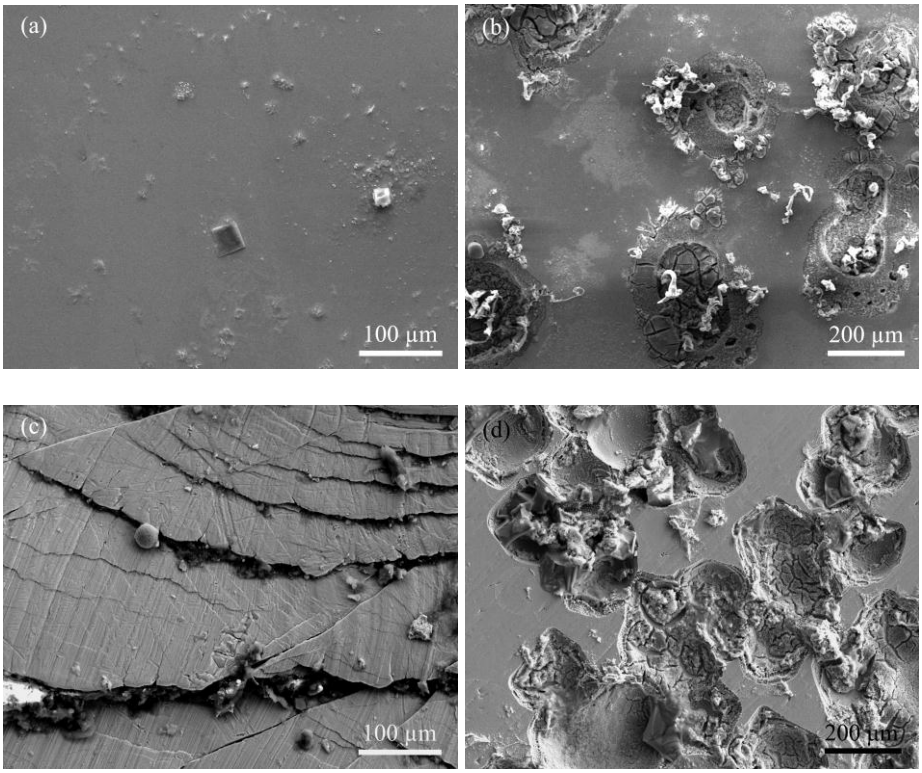

Figure 5. SEM images of the surface for the corroded specimens with different ε rolled at 1×10^{-1} s^{-1}: ε=0 (a), ε=60% (b), ε=95% (d); (c) is the cross section of specimen with ε=60%.

As mentioned above, no phase transformation takes place in the specimen during the whole rolling. Therefore the possibility for deformation-induced nanocrystallization or structural heterogeneous to contribute to decreasing corrosion resistance can be ruled out. The corrosion results raise an intriguing question that what factors contribute to deteriorating the corrosion resistance of the

specimen. Plastic deformation of BMG is known to be inhomogeneous with formation of highly localized shear bands under temperatures far below glass transition temperature, realized by a series of atomic diffusional jumps associated with free volume [13]. Deformation induced free volume as structural defect not only affects mechanical and physical properties [14-17], but also influences corrosion behaviors. Jiang et al. [18] reported that a decrease in free volume by annealing BMG favors the improvement of corrosion resistance. Therefore, it is necessary to scrutinize the free volume content evolution upon deformation，in order to investigate the relationship between the amount of free volume and the corrosion behaviors of the BMGs.

Free volume in metallic glass can be characterized by positron-annihilation spectroscopy (PAS) [19], density measurements [20], and differential scanning calorimetry (DSC) [21]. Here, exothermic peak below T_g (relaxation energy) was used to quantify the free volume content of the BMG, which was developed by Beukel and Sietsma [22]. Fig. 6 shows the relative change of the apparent specific heat ΔC_p calculated from the DSC curves, based on which the variation of the relaxation energies E_r with thickness reductions of the specimens is deduced and shown in Fig. 7.

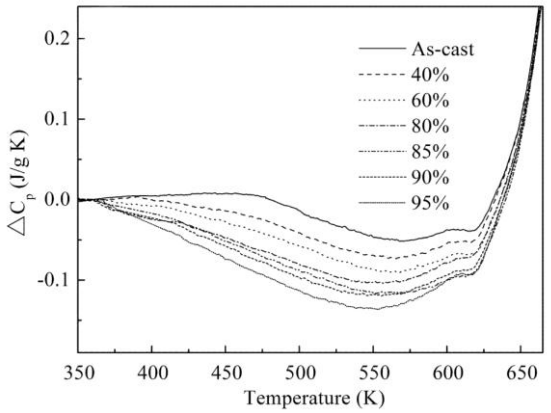

Figure 6. Specific heat data of the specimens with different ε at the strain rate of 1×10^{-1} s^{-1}.

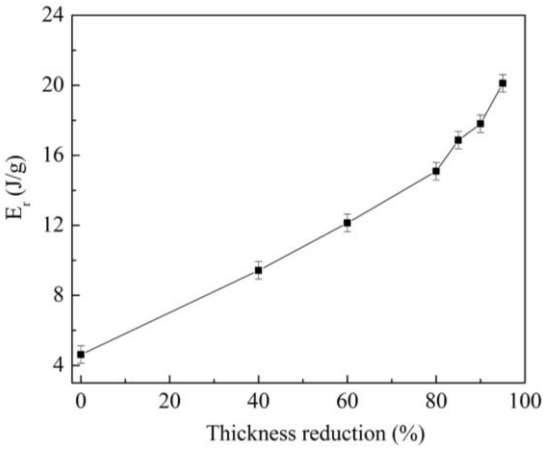

Figure 7. Variation of the relaxation enthalpy per unit mass (E_r) with ε.

It is clear that the E_r monotonically increases from 4.6 to 20.1 $J \cdot g^{-1}$ for the specimens rolled at the strain rate of 1×10^{-1} s^{-1} as ε increases from 0 to 95%, meaning that more free volume is introduced into the as-rolled specimens.

In the present work, no phase transformation occurs in the $Zr_{62}Cu_{12.5}Ni_{10}Al_{7.5}Ag_8$ BMG during rolling. The as-rolled specimens can be considered to be composed of shear bands and the undeformed matrix [23]. The plastic strain mainly concentrated in the shear bands results in rolling-induced free volume mostly stored in them. The introduction of free volume in the shear band increases the average atomic distance [24], and enhances atomic mobility and chemical activity, which puts the amorphous atoms to be a higher energy state and make it susceptible to chemical attack. Consequently, shear bands are sensitive or active sites for pitting corrosion, which has been observed in Zr-Cu-Ni-Al alloy system [25]. As the rolling deformation proceeds, the density of shear bands increases. Considering that the free volume content in a deformed BMG is closely related with the density of shear bands, more free volume is introduced into the metallic glass, and makes the BMG to be higher energy level of metastability, which favors the initiation of pitting corrosion, and fast pit propagation takes place at the motivation of high potential. As a result, the corrosion resistance of deformed BMG significantly decreases with thickness reduction.

As mentioned above, the increase of free volume in the rolled specimen results in deteriorating corrosion resistance. On the contrary, if the rolled specimen was annealed below the glass transition temperature, as shown in Fig 8, compared with the rolled specimen, annealing treatment increases corrosion potential, and shifts polarization curve to lower corrosion current position, bringing about a decrease of I_{corr} from 1.3×10^{-6} $A \cdot cm^{-2}$ for the specimen with ε=95% down to 2.2×10^{-7} $A \cdot cm^{-2}$ for the rolled/annealed specimen with ε=95%, meaning that the rolled/annealed specimen show less spontaneous corrosion tendency and better corrosion resistance. The enhancement of corrosion resistance is originated from structural relaxation associated with the decrease of free volume by annealing which decreases the average atomic distance and atomic mobility, and puts the atoms in the BMG to be lower energy wells, and makes them less electrochemically active. The present work reveals that annealing treatment is an effective way to improve the corrosion resistance of deformed BMGs.

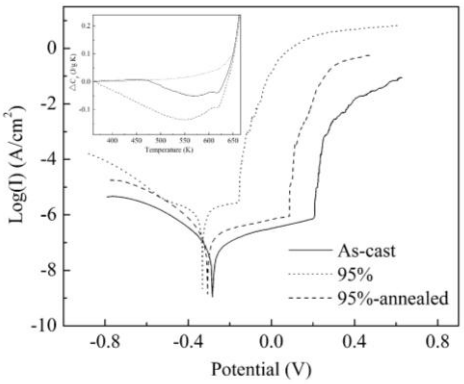

Figure 8. Polarization curves for $Zr_{62}Cu_{12.5}Ni_{10}Al_{7.5}Ag_8$ alloy in the as-cast condition, rolled up to ε=95%, annealed at 638 K for 10 s after rolling up to ε=95%. The annealed specimen was heated by a vacuum electric resistance furnace up to (T_g-10 K), and then cooled down quickly to make sure that no crystallization occurred in the material.

4. CONCLUSIONS

(1) The $Zr_{62}Cu_{12.5}Ni_{10}Al_{7.5}Ag_8$ BMG has been rolled at the strain rate of 1×10^{-1} s^{-1}, to different thickness reductions. The microstructure of the BMG is fairly stable upon rolling deformation. Neither phase separation nor nanocrystalline phase formation has been observed except for the appearance of some localized shear bands in the deformed BMG.

(2) As the thickness reduction increases, the corrosion potential of the BMG shifts to more negative value, and the corrosion current density gradually decreases. Combined with the corrosion morphologies, corrosion reaction in the deformed BMG with large strain is more severe than that of low strain, because it exhibits an increase in free volume content during the rolling. It is proposed that free volume mainly concentrated in shear band increases the pitting susceptibility, leading to the reduction of corrosion resistance. Nevertheless, the corrosion resistance in the rolled specimen can be enhanced by relaxation annealing associated with annihilation of free volume.

ACKNOWLEDGEMENT
This work is financially supported by the National Natural Science Foundation of China (Nos. 51401139 and 51204115), the Natural Science Foundation of Jiangsu Province (Nos. BK20141193 and BK20130304) and the China Postdoctoral Science Foundation (No. 2013M541719).

References

1. W.H. Wang, C. Dong, C.H. Shek, *Mater. Sci. Eng*. R, 44 (2004) 45-89.
2. C.A. Schuh, T.C. Hufnagel, U. Ramamurty, *Acta Mater*., 12 (2007) 4067-4109.
3. J.J. Si, T. Wang, Y.D. Wu, Y.H. Cai, X.H. Chen, W.Y. Wang, Z.K. Liu, X.D. Hui, *Appl. Phys. Lett.*, 106 (2015) 251905.
4. J.M. Yin, H.N. Cai, X.W. Cheng, X.Q. Zhang, *J. Alloys Comp*., 648 (2015) 276-279.
5. A.H. Taghvaei, M. Stoica, K.G. Prashanth, J. Eckert, *Acta Mater*., 61 (2013) 6609-6621.
6. P.F. Gostin, A. Gebert, L. Schultz, *Corros. Sci.*, 52 (2010) 273-281.
7. X. Wang, Q.P. Cao, Y.M. Chen, K. Hono, C. Zhong, Q.K. Jiang, X.P. Nie, L.Y. Chen, X.D. Wang, J.Z. Jiang, *Acta Mater*., 59 (2011) 1037-1047.
8. Q.P. Cao, J.F. Li, Y. Hu, A. Horsewell, J.Z. Jiang, Y.H. Zhou, *Mater. Sci. Eng*. A, 457(2007) 94-99.
9. M.H. Lee, D.H. Bae, D.H. Kim, W.T. Kim, D.J. Sordelet, K.B. Kim, J. Eckert, *Scripta Mater*., 58 (2008) 651-654.
10. K.C. Hwang, E.S. Park, M.Y. Huh, H.J. Kim, J.C. Bae, *Intermetallics*, 18(2010) 1912-1915.
11. P.N. Zhang, J.F. Li, Y. Hu, Y.H. Zhou, *J. Mater. Sci*., 43(2008) 7179-7183.
12. W. Zhou, X. Lin, J.F. Li, *J. Alloys Comp*., 552 (2013) 102-106.
13. F. Spaepen, *Acta Metall*., 25 (1977) 407-415.
14. Y.J. Huang, F.L. He, H.B. Fan, J. Shen, *Scripta Mater*., 67 (2012) 661-664.
15. N. Adachi, Y. Todaka, Y. Yokoyama, M. Umemoto, *Appl. Phys. Lett*., 105 (2014) 131910.
16. D. Singh, R.K. Mandal, R.S. Tiwari, O.N. Srivastava, *J. Alloys Comp*., 648 (2015) 456-462.
17. S. Gonzalez, E. Pellicer. S. Surinach, M.D. Baro, J. Sort, *Intermetallics*, 28 (2012) 149-155.
18. W.H. Jiang, F. Jiang, B.A. Green, F.X. Liu, P.K. Liaw, H. Choo, K.Q. Qiu, *Appl. Phys. Lett.*, 106 (2015) 251905.
19. K.M. Flores, E. Sherer, A. Bharathula, *Acta Mater*., 55 (2007) 3403-3411.
20. Y. Zhang, H. Hahn, *J. Non-Cryst. Solids*, 357 (2011) 1420-1425.

21. B.P. Kanungo, S.C. Glade, P.A. Kumar, *Intermetallics*, 12 (2004) 1073-1080.
22. A. van den Beukel, J. Sietsma, *Acta Metall.*, 38 (1990) 383-389.
23. H. Bei, S. Xie, E.P. George, *Phys. Rev. Lett.*, 96 (2006) 105503.
24. M.S. Pham, K.W. Park, B.G. Yoo, J.I. Jang, J.C. Lee, *Met. Mater. Int.*, 15 (2009) 209-214.
25. X.P. Nie, Q.P. Cao, Z.F. Wu, Y. Ma, X.D. Wang, S.Q. Ding, J.Z. Jiang, *Scripta Mater.*, 67 (2012) 376-379.